IOSR Journal of Applied Geology and Geophysics (IOSR-JAGG)
e-ISSN: 2321–0990, p-ISSN: 2321–0982.Volume 10, Issue 1 Ser. II (Jan. – Feb. 2022), PP 18-28
www.iosrjournals.org

Petrological and Geochemical Evaluation of the Otutu Rift Segment, Kenya

Erique O. Nyawir [1, 2*], Jacques Varet[2], Peter O. Omenda[3]
[1]*Kenya Electricity Generating Company, Kenya*
[2] *Geothermal Training and Research Institute, and Dedan Kimathi University of Technology (DeKUT), Kenya*
[3] *Managing Director at Scientific and Engineering Power Consultants (SEPCO), Kenya*
**Corresponding author: Erique O. Nyawir*

Abstract: *Otutu rift segment lies in between the Eburru and Elmenteita volcanic field within the Kenya Central Rift Valley. It is one of the areas within the Kenyan rift that has not been fully explored nor developed geothermally. Rock samples were collected from the study area with an intention of acquiring more information on the surface mineralogical and chemical characteristics of the volcanic lavas within the study area. The area was selected as a representative of an active rift segment of the Kenya Rift Valley (KRV). This information assisted in the understanding of the origin and evolution of the magmas. Magmatic events in geothermal areas provide irreplaceable tools to characterize heat sources which are one of the key things being looked for during geothermal prospecting: the other factors being permeability, water recharge system, presence of both reservoir and cap rocks. Petrological investigations allowed to identify a large variety of lava rocks, ranging from alkali olivine basalts to mugearites, trachytes and pantelleritic obsidians, with a relative abundance of the last. Geochemical analysis carried on the selected fresh aphyric rock samples provided a complete view of the various kind of liquids emitted during the last million years along this active segment of the rift. A variety of volcanic products were emitted during each of the successive steps of the rift segment development, each ranging from alkali-olivine basalts to pantellerites, with a few intermediate types. Geochemical analysis of the rocks show that this evolution can be simply explained by a process of crystal fractionation occurring in the crust a few kilometres deep. These results are of interest for the future development of the area, as well as – more generally – the search for new geothermal resources along the East African Rift System away from the central volcanic units along other active rifts segments which represent much wider areas than the ones presently being targeted.*

Date of Submission: 16-01-2022 Date of Acceptance: 31-01-2022

I. Introduction

The study area, Otutu rift segment, lies in between the Eburru-Elmenteita volcanic field and is part of the active rift segment in Kenya that is located between two main central volcanic centres, namely, Olkaria and Menengai. The field is in the central part of the Kenya Rift Valley (KRV) which is part of the East African Rift System (EARS), one of the great African features, a tectonic feature caused by the earth's crust fracturing. The EARS is part of the main active rift zone that connects at the Afar triangle to the Red Sea and Gulf of Aden Oceanic rifts and extends down south to central Mozambique (Figure 1). In its median part, the EARS is made up of two main rift segments: the Eastern and the Western Branches. From north to South, the spreading rate decreases along the Eastern Rift whereas it increases along the western rift, Chorowicz (2005). The Kenya Electricity Generating Company, PLC (KenGen) together with Geothermal Development Company (GDC) have been exploring for geothermal energy resources in the country to provide environmentally clean and low-cost energy for the country. KenGen is currently producing electricity from geothermal resources at Olkaria and Eburru while GDC is undertaking production drilling in Menengai and has commenced exploratory drilling further north in Paka volcano, Omenda and Simiyu (2015). Additionally, the government of Kenya has licensed several geothermal areas to private investors to explore and develop the resources for power generation and direct use.

The main objective of this project was to undertake petrological and petrochemical studies of the Otutu rift segment that lies in between the Eburru and Elmenteita volcanic fields within the Kenya Rift Valley. This study area is herein referred to as the Otutu Rift Segment as it encompasses the area on the rift floor that includes the Recent Aa lava flow in Badlands. The study's main intention is to acquire more information on the surface mineralogical and chemical characteristics of the volcanic lavas and relate the characteristics to magmatic evolution of the eruptive products.

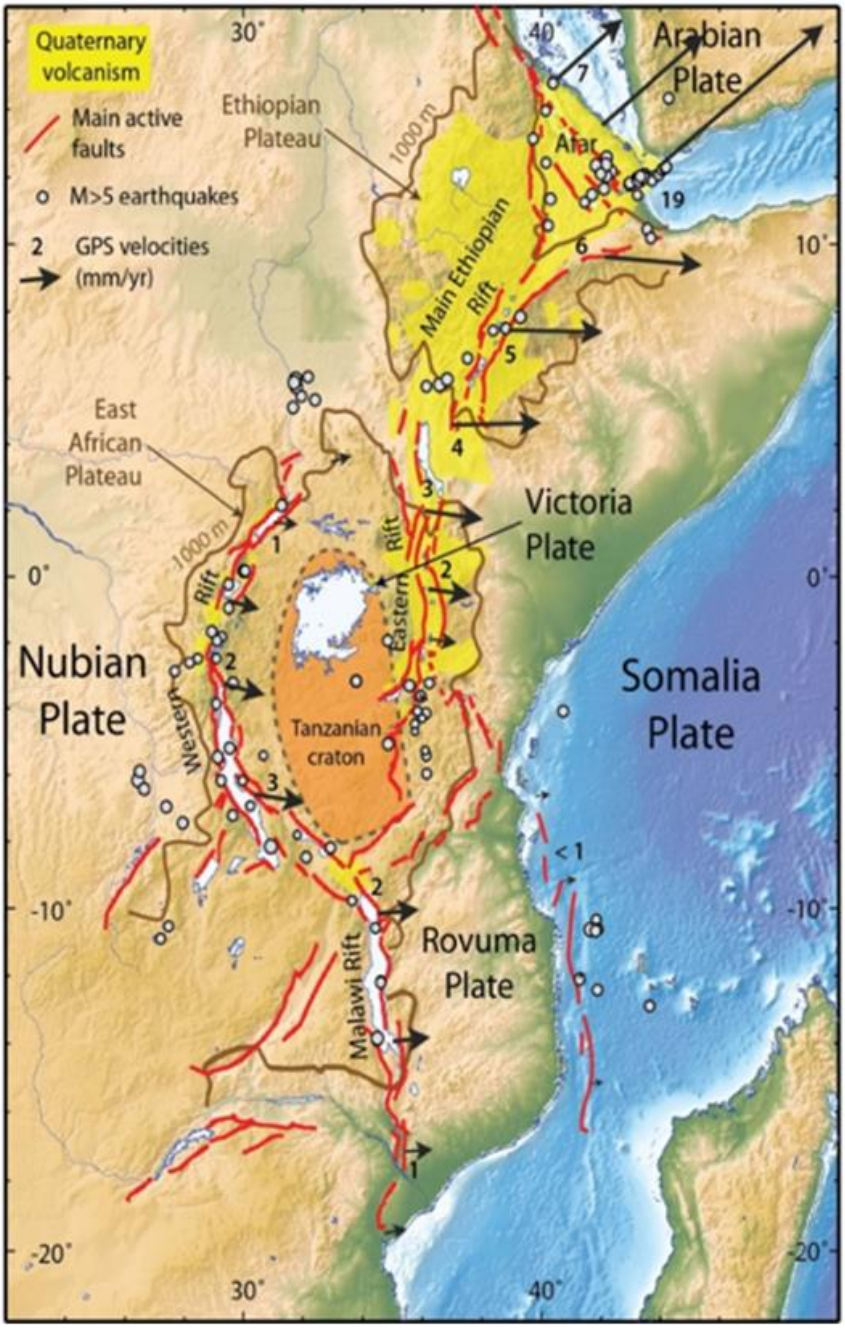

Figure 1: The East African Rift System showing major fault systems (in red), Quaternary volcanism (in yellow) and associated seismicity (M>5). Plate-motion vectors with GPS velocities (mm/y) are also indicated (Calais et al, 2006).

II. Problem Statement

Several geoscientific studies have been undertaken in the Kenya Central Rift since early 1960s. These studies have included geological, hydrogeological, geophysical, and geochemical, amongst other studies and have mostly concentrated on the numerous volcanic centres (central volcanoes) that lie in the KRV like Longonot, Suswa, Olkaria, Eburru and Menengai. The rift floor, including the Otutu rift segment, has not been studied comprehensively in terms of detailed petrographic and petrochemical study of the lava suite as much as the volcanic centres that are characterized by spectacular structures in the Kenya Central Rift. This research focused on a detailed study of this rift segment that is located between the Eburru central volcano and Lake Elmenteita. From this study it was possible to understand the various geological structures, the possible magma sources for the lava there and how the volcanic units offered the evolutionary processes that resulted in the generation of the various range of lava that appear on the surface of the study area. This is an important case study as it can be used to understand the petrogenesis of the rock types in the area as well as deduce the dyke

system in the area that fed the young lava flows and domes: if the diversity of lava types can be explained by fractional crystallization, this supports the existence of magma chambers, and this could possibly mean an existence of a local geothermal resource. This knowledge can also be used to characterize the whole KRV and MER areas as it is a good representative of an active continental rift.

III. Methodology

This research work entailed desktop study, fieldwork, sample collection, preparation, analysis, data interpretation and report writing (Figure 2). Desktop study was undertaken by carrying out literature review of the study area and the subject of interest (geology, petrology, and petrochemistry). Maps and aerial images of the study areas were studied in depth, and this assisted in identifying the different outcrops and structures in the study area. This was then followed by identification of the most relevant sites to visit, site reconnaissance, and finally fieldwork that included detailed observations in the field as well as sample collection. The surface rock samples from the prospect area were collected from the field by traversing across and along the area. All the locations of the sampling sites were recorded using a GPS The samples collected were subjected to preliminary checks and observation and thereafter taken to the laboratory for more detailed analysis. These analyses included petrographic description of the rocks and their thin sections as well as a detailed petrochemical analyses.

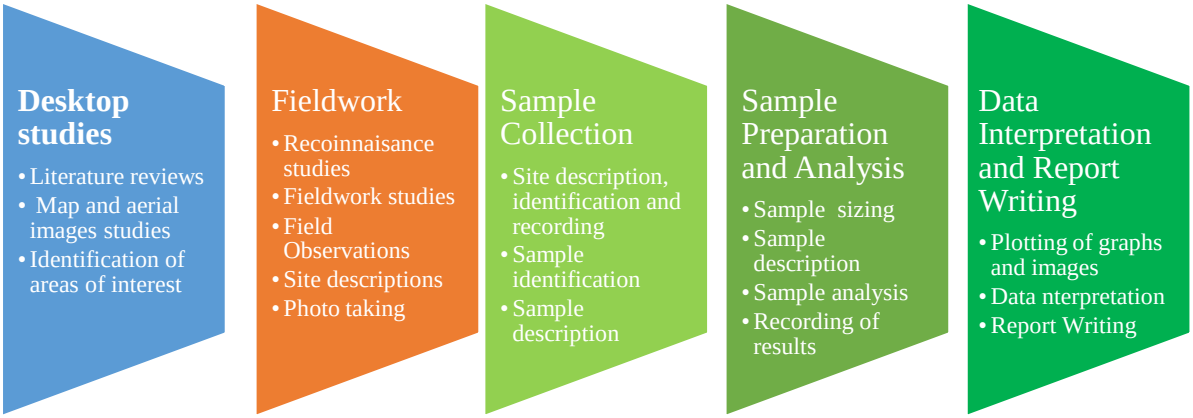

Figure 2: Schematic representation of the research methodology

Petrographic analysis was used to study the mineralogical evolution, confirm the rock type(s), the alteration minerals, and any additional alteration minerals not observed by the binocular microscope or the hands lens. For petrographic microscope analysis, thin sections were prepared at KenGen's Geology lapidary laboratory in Olkaria, Kenya. These thin sections were analysed in both KenGen' s Geology Laboratory in Kenya and the BRGM laboratory in France using Optika B-353POL and the LEICA DM 4500P Microscope respectively. However, the whole rock analysis involving both major and trace/rare elements analysis was carried out by use of ICP-MS and ICP-AES in UBO, Brest, France.

IV. Results and Discussion

The 120 rock samples obtained from the fieldwork (Figure 3) were analysed petrographically, both in the field (study area) and in the lapidary laboratories at KenGen, Olkaria (Naivasha, Kenya) and later at BRGM, Orleans (France). Thereafter 21 samples were carefully selected and subjected to rock geochemistry at IUEM, UBO in Plouzané, Brest, France. From this analysis, the major and trace elements contents of the rock samples were obtained and are well tabulated in Appendix II. Additional data of the study area was obtained from 13 samples results borrowed from Omenda (1997).

The samples were grouped into 3 distinct categories: Basalts (Lower and Upper Elmenteita), Trachytes (Pliocene Gilgil and Eburru shield-building trachytes) and rhyolites (pantellerite).

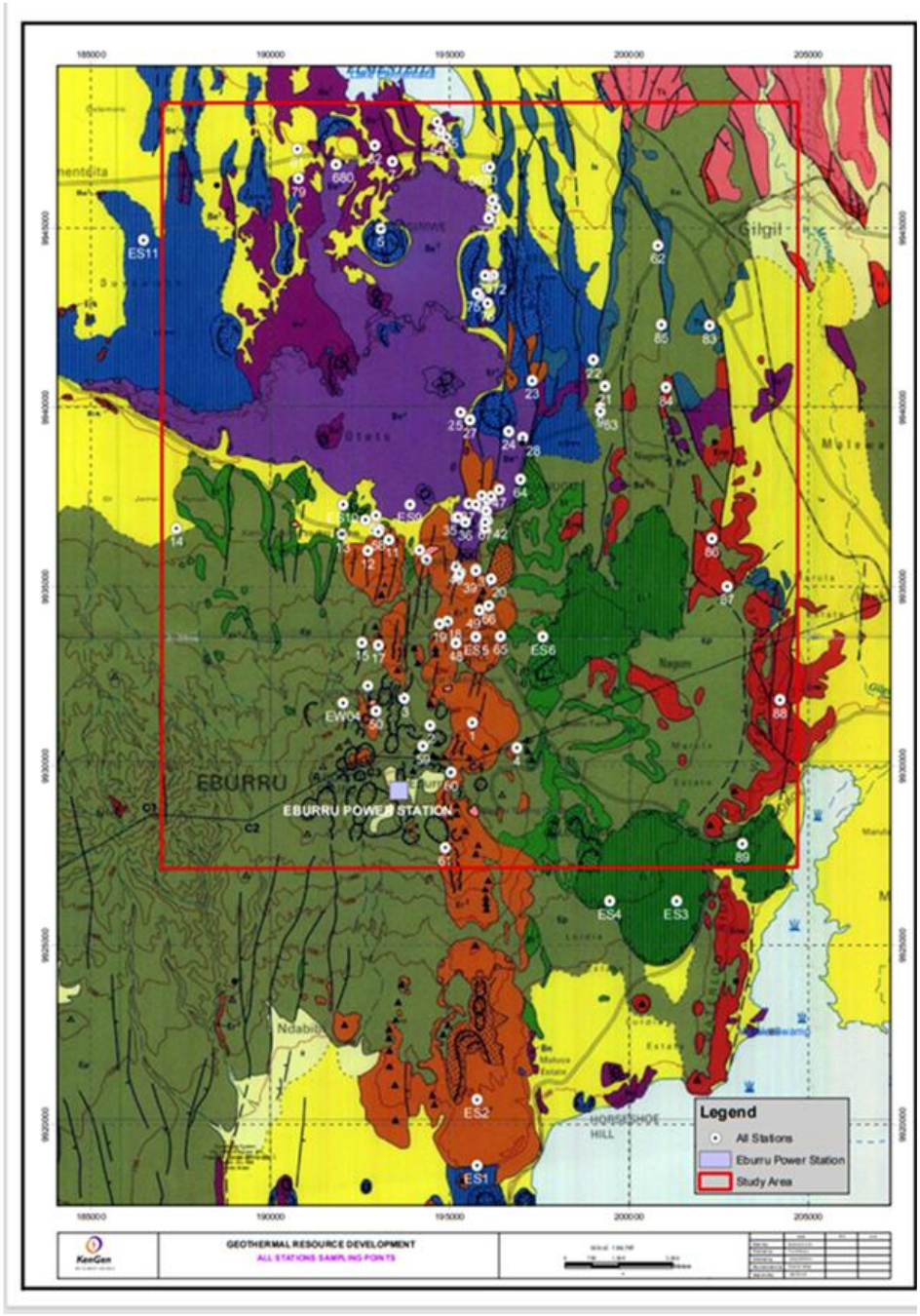

Figure 3: The study area earmarked by the red rectangle while the mapped stations in dotted white (Adapted from Clarke et al., 1990).

(a) Total Alkali Silica classification

The Total Alkali-Silica diagram is very important in classification of igneous rocks. It classifies the volcanic rocks into different rock types based on their silicic and alkali content, LeBas et al (1986). The total alkali and silica values were normalized to 100% before being plotted in the TAS Diagram. From Figure 4, the TAS Diagram shows a regular trend for all samples, slightly above the alkaline / sub-alkaline dividing line (dotted red on the diagram below) which is typical for all transitional series found elsewhere in the EARV including Afar (Barberi et al, 1975). The rock sampled ranged from mafic through intermediate to silicic rocks (basalts, trachy-basalts, basaltic trachy-andesites, trachy-andesites, trachytes to rhyolites).

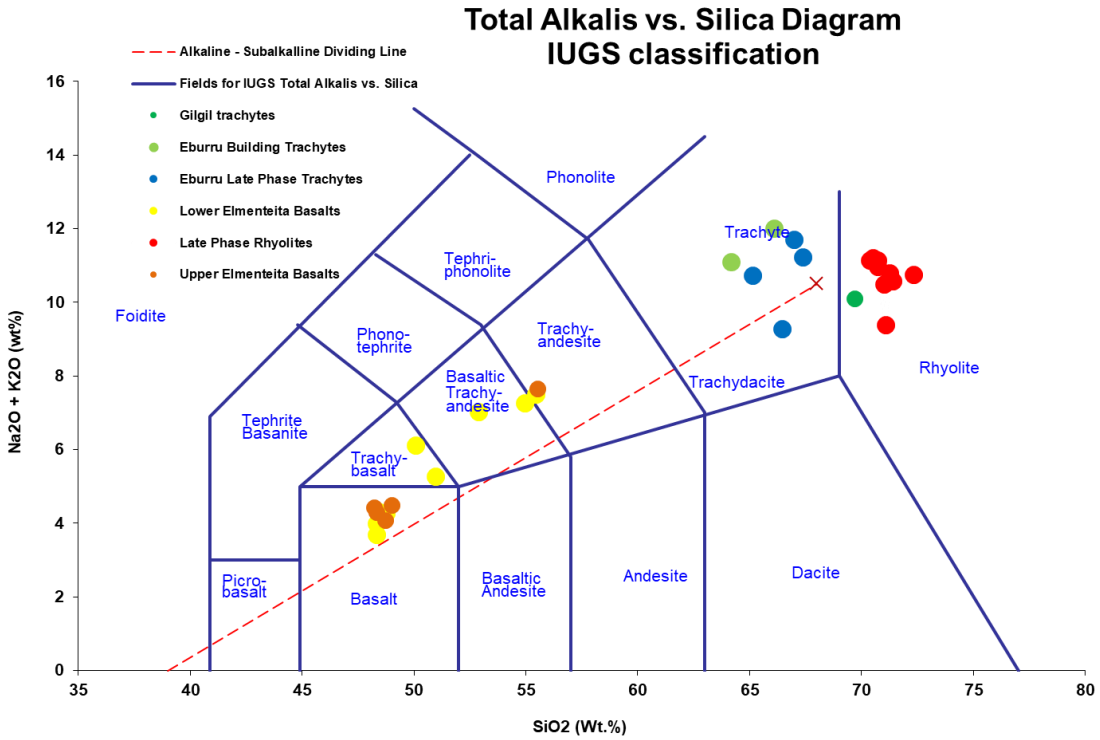

Figure 4: Total Alkali vs Silica Diagram for the study area

Lower Elmenteita basalts vary in composition from basalt through trachy-basalt to basaltic trachy-andesite. Their alkali content varies from 3.69 to 7.51% while their silica content varies from 48.31 to 55.46%. All the upper Elmenteita basalts samples except sample EN/EBLE 25A fall under the basalt category. Their normalized silica content varies from 48-49% with the alkalis part ranging from 4.09-4.49%. Sample EN/EBLE 25A has a relatively high silica content (55.1%) with also relatively high alkalis (7.66%).

Generally, the Upper Elmenteita basalts are low in both silica and alkali compared to the Lower Elmenteita basalts. They have a general composition of 45-52% SiO_2 and 2 to 5% alkalis. This is noted in the upper Elmenteita suite but apparently the lower Elmenteita suite seems to be higher in their silica and alkali content. This varying composition noted in this basaltic suite (lower Elmenteita) could be as a result of fractional melting.

The one sample of Gilgil trachyte have high SiO_2 (69.67%) which make it fall within the rhyolite field. However, petrographic analysis clearly indicates that the lava is a trachyte. The lava has an alkali content of 10.12%. Eburru shield trachytes all fell under the trachytes. They had alkali concentrations of 9.3-11.2% with silica content ranging from 64.2 to 67.4%.

Generally, trachytes are feldspar-rich and thus have 60-65% silica content and averagely 7% alkali. Most of the samples had high silica and alkalic content and plotted towards the tail end of the trachyte portion in the TAS Diagram.

Rhyolite plot with an alkali content of 9.4 to 11.2% while the silica content was 70.4-71.4%. This is expected of rhyolites as they are the most silica rich igneous rocks. They usually have higher SiO_2 (69-77%) and alkali (>7%).

All the trachyte and rhyolite suites are all silica saturated with concentrations ranging between 64.18 and 71.4% by weight. The suites have also relatively high alkali contents that range between 9.3 to 11.2% and 9.4 to 11.2% by weight, respectively.

Therefore, all the samples plotted above the line that separates the alkaline and sub-alkaline rocks (Figure 4). This means all the rocks are alkaline rocks. Alkaline magmas are known to be derived from the mantle-derived basaltic melts, Bailey (1987). These melts usually have had residence in the crust and thereafter evolve through the assimilation and fractional crystallization (AFC) processes.

(b) AFM classification

The AFM Diagram is used for showing relative portions of rock oxides and takes its name from the oxides plotted at its apices- Alkalis (Na_2O + K_2O), Fe oxides (FeO + Fe_2O_3) and MgO (Rollinson, 1993). Though it is widely used in mafic rocks, it also works well with the more silicic volcanic rocks. AFM Diagrams, in their classification, distinguishes between the two usual types of parental magmas: alkali and tholeiitic

(Figure 5). It is noted that the lavas evolved through depletion of Fe and Mg and enrichment of alkalis. All the samples plotted below the Tholeiitic (sub-alkaline) series. It is noted that tholeiitic magmas usually form at relatively shallow depths compared to alkalic magmas and differentiate into the SiO_2 oversaturated rhyolites.

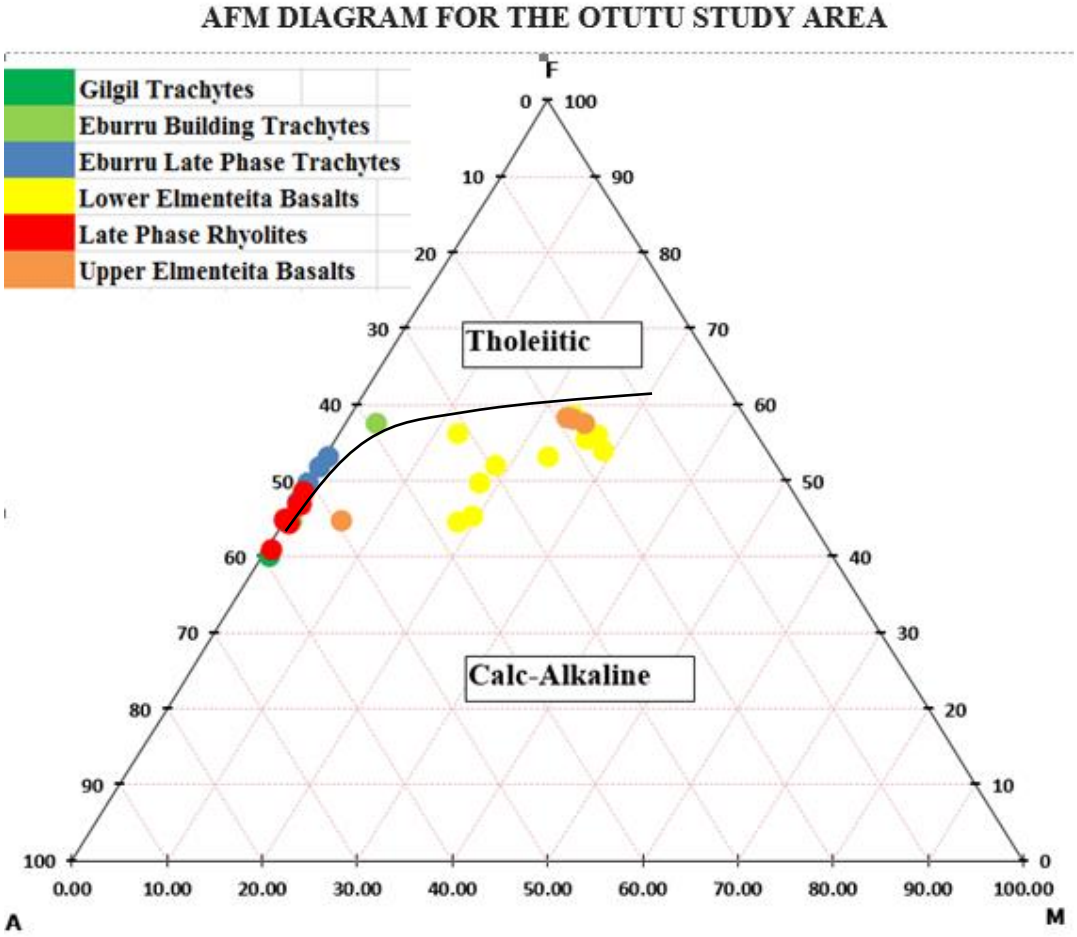

Figure 5: AFM Diagram for the Otutu study area

Figure 5 shows both trachytic and rhyolitic lavas plotting on the zero MgO axis due to their very low MgO contents while having high contents of alkali and Fe. The evolution of the Elmenteita and Eburru lavas can be described by the fractional crystallization process involving crystallization of ferromagnesian minerals (olivine and pyroxenes) as shown by decreasing Mg and Fe with evolution from basalt through trachyte to rhyolite. The evolution is characterized by enrichment of alkalis in the liquid phase.

c) Variation diagrams

Harker variation diagrams are used to test co-genetic lavas and evolutionary processes. This is done by plotting various oxides against SiO_2 (on the x-axis). SiO_2 is preferred as a differentiation index as it has high concentration and is incompatible to an extent. SiO2 is the best measure of differentiation for rocks with > 50% SiO2 and less than 6% MgO, Hochstaedter et al, 2000. It also has a wide variation in the common lavas from about 45% in mafics to over 70% in silicic rocks. Lavas that are cogenetic are expected to show strong correlation when the oxides are plotted on a binary diagram.

Whereas Upper Elmenteita basalts are younger than the Lower Elmenteita Basalts, they have the highest TiO_2 contents. The graph of SiO_2 vs TiO_2 shows decreasing TiO_2 content from basaltic lava through intermediate lavas to rhyolite (Figure 6). The trend suggests fractionation of magnetite and/or ilmenite during evolution of the lavas from basalt to rhyolite. The trend further suggests that the Upper Elmenteita basalts could not be cogenetic with the stratigraphically Lower Elmenteita basalts since they are less evolved.

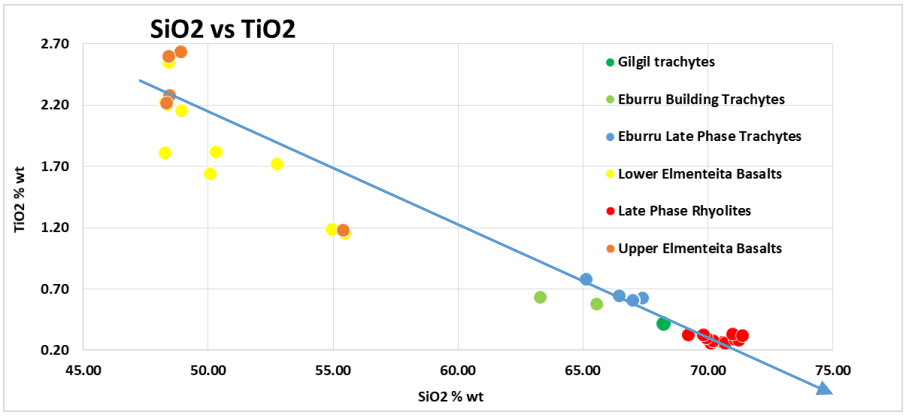

Figure 6: SiO_2 vs TiO_2 variation diagram

Plot of SiO_2 vs MgO shows that the basalts at Elmenteita are moderately evolved with SiO_2 of 48-55% and MgO contents of between 3.7% and 6.5% (Figure 7). The Lower Elmenteita basalts have some samples with the highest MgO content but show a wide range indicating that the various lava flows are products of different degrees of differentiation. The upper Elmenteita basalts also have SiO_2 of 48-55% but with MgO contents of 3.8 to 6.0%. The wide spread within the Upper basalts indicates that the lava field comprise a suite of rocks that experienced varied degrees of fractional crystallization. The trachytes and rhyolites have very low MgO suggesting that they are products of protracted fractional crystallization from basaltic liquids.

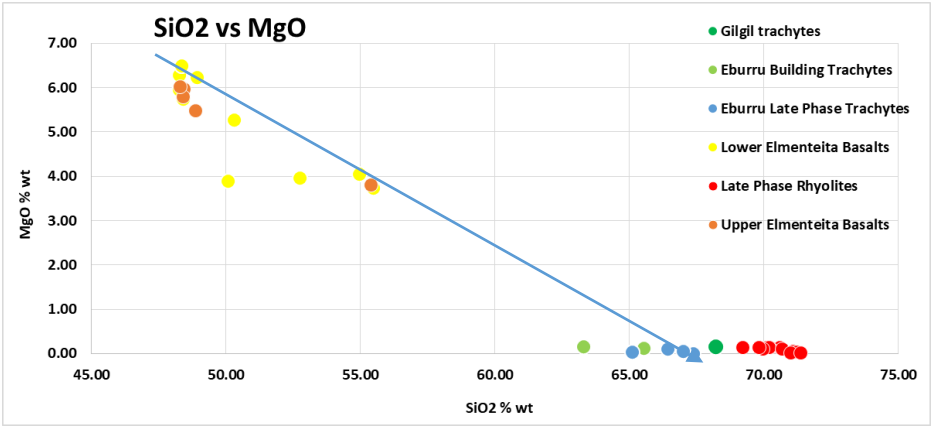

Figure 7: SiO_2 vs MgO variation diagram

Alumina (Al_2O_3) plot of the study area shows highest values within the Lower Elmenteita basalts followed by the Upper Elmenteita basalts. However, there is quite a scatter in the plot of the basalts attributed to incorporation of feldspar crystals in the analysed bulk samples (Figure 8). The plot shows decreasing trend of Al_2O_3 with increasing SiO_2 with the lowest values in rhyolites and this indicates role of feldspar fractionation in the evolution of trachytes and rhyolites.

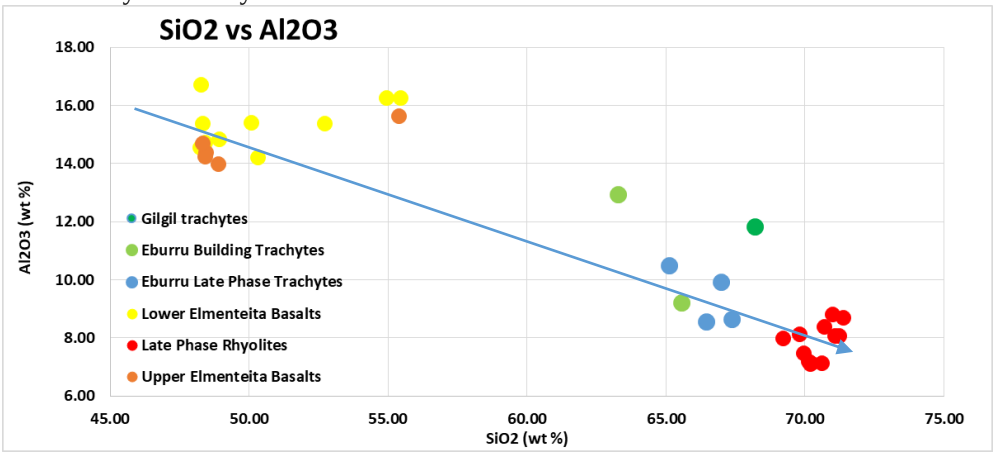

Figure 8: SiO2 vs Al2O3 variation diagram

Variation of total Fe_2O_3 with SiO_2 shows decreasing contents with increasing silica (Figure 9). However, the basalts show a scatter without any clear trends amongst the suites. Rhyolites have the lowest contents, and the data is inconclusive as the basalts seems to fall in a different part of the graph when compared with the trachyte and rhyolites. However, the plot can be interpreted to indicate that trachytes and rhyolites can be generated from basalts by fractionation of Fe-oxide minerals.

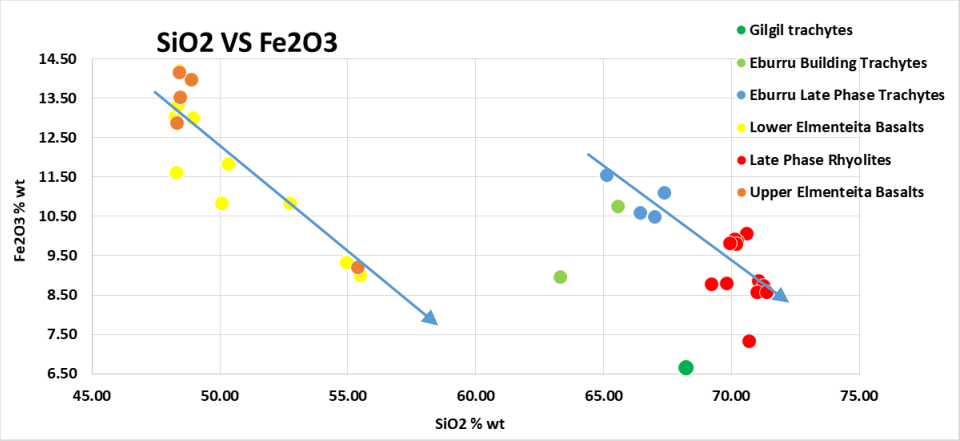

Figure 9: SiO2 vs Fe2O3 variation diagram

SiO_2 vs CaO shows a clear reducing trend from basalts through trachyte to rhyolite (Figure 10). The graph shows a linear trend within the Lower Elmenteita suite further confirming that the group has several flows that may be related through fractional crystallization process. It can be postulated that the cause of the observed trend is fractionation of calc-plagioclases. Extreme fractional crystallization from trachyte to rhyolites with calc-plagioclases, among other minerals, resulted in the very low values of CaO in the rhyolites.

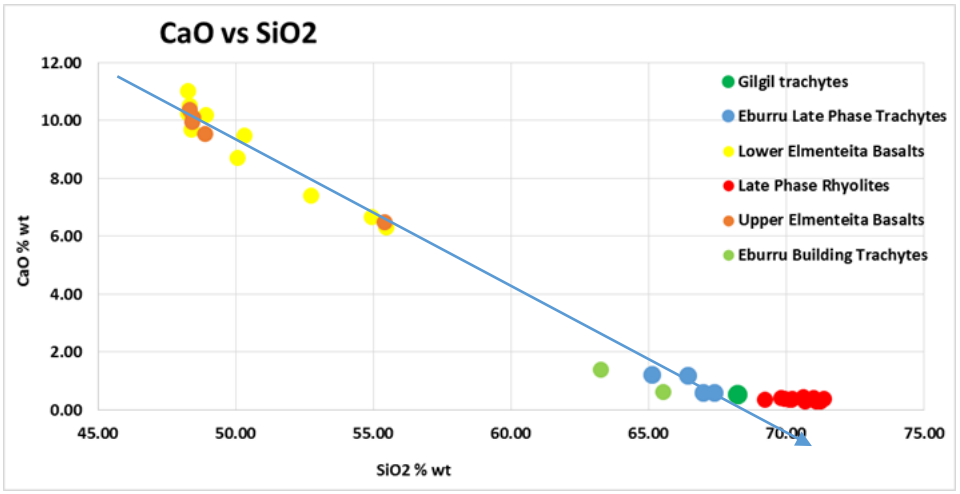

Figure 10: SiO_2 vs CaO variation diagram

P_2O_5 variation with SiO_2 shows highest values among the Upper and Lower Elmenteita basalts (Figure 11). P_2O_5 shows a wide linear variation with the Lower Elmenteita basalts suggesting that the lavas that form the formation are related amongst themselves via fractional crystallization. The phosphorus decrease is due to the crystallisation of apatite. Trachytes and rhyolites are very low P_2O_5 contents which therefore are not in trend with the basalts.

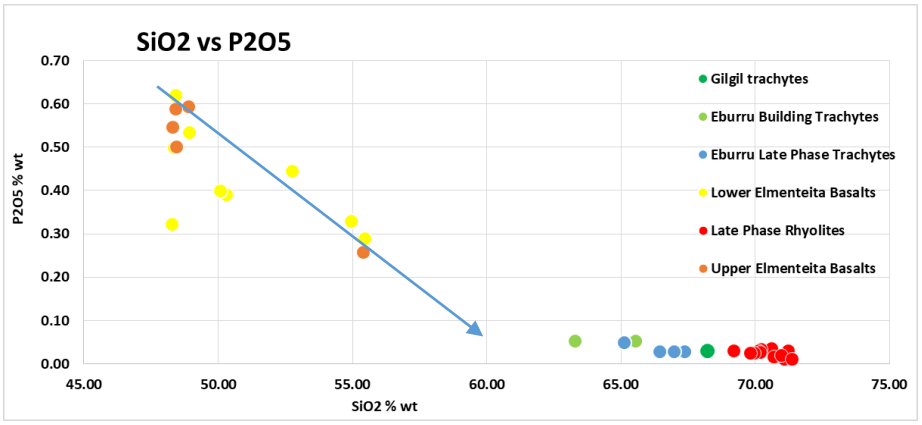

Figure 11: SiO_2 vs P_2O_5 variation diagram

Na_2O and K_2O behaves incompatibly during fractional crystallization of liquids from basalts to trachytes and rhyolites and therefore its contents increase with SiO_2 (Figures 12 and 13).

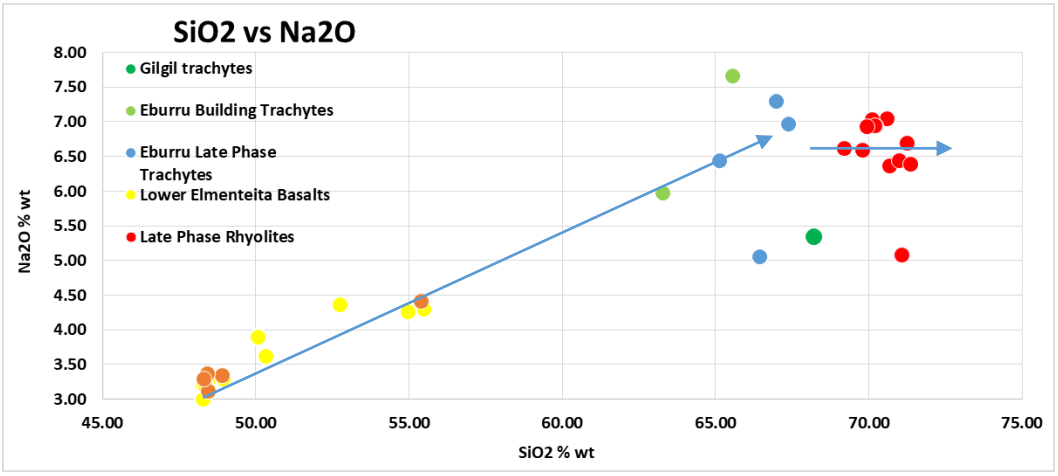

Figure 12: SiO_2 vs Na_2O variation diagram

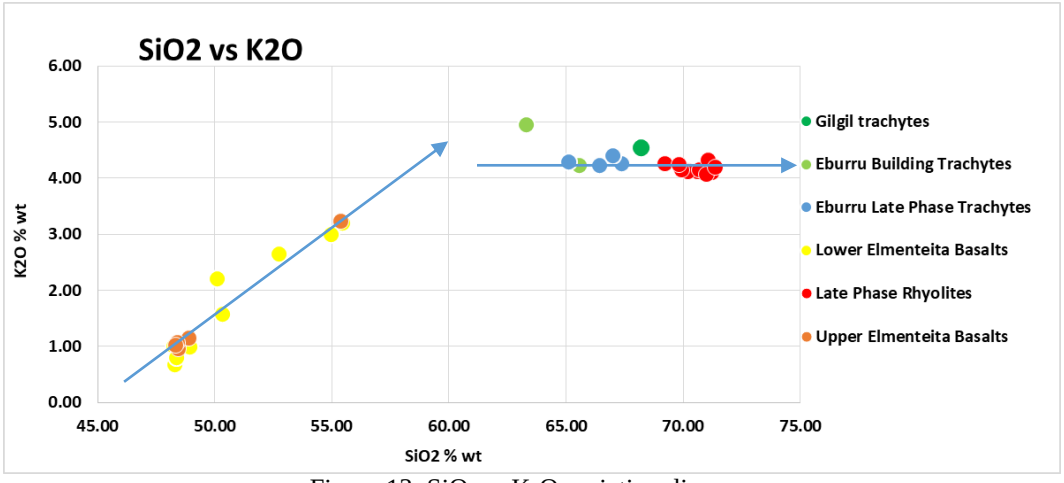

Figure 13: SiO_2 vs K_2O variation diagram

The strongest incompatibility is recognized from basalts to trachytes where linear trends are observable. This trend can be attributed to the highly incompatible nature of Na2O which results in its enrichment. However, flattening of the curves is noted between trachyte and rhyolite which can be attributed to fractionation of feldspars.

It is, generally noted, as in other rift magmatic sequence, that alkalis and silica clearly increase in the successive rocks (liquids) of the study area, whereas magnesium, calcium, aluminium, iron and titanium

decrease after a slight initial increase. This is as a result of the fractional crystallization of olivine, pyroxene, the calcium-rich plagioclase (observed as phenocrysts in nearly the whole rock sequence with exemption of the pantellerites), and more seldom the amphiboles (with iron oxides around oxidation rims). This noted negative correlation is also attributed to the fractionation of iron, titanium, and aluminium-bearing minerals e.g. the olivine and clinopyroxene, Fe-Ti oxides, and plagioclase respectively.

The regular calcium and aluminium oxide decrease confirm here the major role played by plagioclase fractionation, whereas olivine, pyroxene and amphibole fractionation explain the magnesium, iron, and titanium decrease. Interesting to note is the slight and slow decrease of potassium at the end of the sequence, which can be interpreted as resulting from sanidine crystal fractionation. And in fact, abundant sanidine phenocrysts were noted in most porphyritic obsidians.

d) CIPW Norm Classification

As classically used in petrological studies, normative composition of the rocks was calculated using CIPW method (CIPW Norm Hollacher, 2014). The resulting normative mineral compositions showed that the rocks samples ranged from transitional basalts to rhyolites in the six identified sub-groups within the Otutu Rift segment.

The basaltic (lower and upper Elmenteita) samples contain no normative quartz but very high values of normative plagioclase and average normative orthoclase. This ranged between 52.4-62.1% and 5.2-22.3%, respectively. The normative diopside ranged from 10-19.5% while the normative olivine values ranged from 4.5 to 12.2%. Normative ilmenite varied from 1.3 to 3.2% and normative magnetite varied from 1.1-18%.

Normative nepheline values were generally low. Values ranging from 0.0 to 3.0% and 0.5 to 1.4% for normative nepheline and apatite, respectively were also noted with most samples containing no normative sodium silicate. Normative leucite was absent from all the basaltic samples, which is expected of all sub-alkaline bulk chemistry. The normative zircon ranged from 0.01 to 0.02% while the normative chromite values were at 0.01%. All the other remaining normative minerals were absent or very low. These included acmite and calcite.

In the trachytic samples, normative quartz was noted. This ranged from 7.8% in sample 13 to 15.9-26.2% in the other samples. The samples also had relatively high values of normative plagioclase and normative orthoclase. This ranged between 22.3-42.3% and 27.7-32.6% respectively. The normative diopside ranged from 1.8 to 4.6%, while the normative hypersthene values ranged from 5.8 to 10%. Normative acmite varied from 2.3 to 3.9% while normative sodium silicate varied from 1.8 to 9.8%. Normative ilmenite was low and varied from 0.34-0.9% while normative magnetite was very low (0.06%) and mostly absent. Normative apatite and zircon values were generally very low. Values ranging from 0.1 to 0.14 % and 0.0 to 0.1 % for normative apatite and zircon were noted respectively. All the other remaining normative minerals were absent or very low. These included accessory minerals like nepheline, olivine, chromite, and calcite.

In the rhyolitic samples, higher normative quartz was noted in comparison to the trachytic samples. This ranged from to 30.0-33.1%. The samples also had relatively high values of normative plagioclase and normative orthoclase. This ranged between 14.5-24% and 26.0-28.2% respectively. The normative diopside was averagely low, ranging from 0.9 to 1.3%, though sample ES1 had 2.7% while the normative hypersthene values ranged from 7.1 to 9.7%. Normative acmite varied from 2.5 to 3.4% while normative sodium silicate was averagely high varying from 5.8 to 11.1%. Normative ilmenite was averagely low and varied from 0.3-0.4% while normative magnetite was very low (0.06%) and mostly absent. Normative apatite and zircon values were generally higher compared to basalts and trachytic suites. Values ranging from 0.02 to 0.08% and 0.18 to 0.24 % for normative apatite and zircon were noted respectively. All the other remaining normative minerals were absent or very low. These included accessory minerals like nepheline, magnetite, olivine, chromite, and calcite.

Generally, by CIPW silicic rocks usually have normative quartz varying from the lower end trachytes through ignimbrites to the higher end rhyolites. The average quartz values are 1-4%, 17-21% and 22-30% for trachytes, ignimbrites, and rhyolites respectively. Silicic rocks also have averagely high values of plagioclase and orthoclase. For silicic rock as a whole, these ranges between 31-55% and 25-30% respectively.

Most of the basalts show a good balance, with both olivine and hypersthene present, but not quartz (no tholeiite) whereas only 3 samples show the presence of nepheline, mostly as traces (ranging from 0.3-0.4%) with only one sample exceeding 1%, which confirm the transitional characteristic of the basaltic magma source. Whereas olivine is always visible in thin sections under the microscope, orthopyroxene is not observed, which is classical in basaltic environment (orthopyroxenes rather appear in plutonic environments). However, during the differentiation process, the magma progressively acquires a slight, then dominant silica saturation in the end products.

Amphiboles are not present in the normative analysis for the simple reason that the CIPW norm is based on "dry" mineral only – pyroxene in this case - and do not allow for amphibole (or mica) to occur. These frequently show signs of instability (mineral internally altered and rimmed with iron oxides) with the groundmass, indicating that these silica-deficient minerals formed at depth are not in equilibrium with the silica-

saturated liquid containing them when emitted at the surface in more oxidizing and eventually "dryer" conditions.

V. Conclusion

Petrological investigations in this research allowed for the identification of the bimodal nature of the rocks in the area. The area had a large variety of both basic and acidic rocks. These variety of lava rocks ranged from alkali olivine basalts to mugearites, trachytes and pantelleritic obsidians, with a relative abundance of the last were noted. Petrological analysis of the rocks and their interpretation show that this evolution can be simply explained by a process of crystal fractionation occurring in the crust a few kilometres deep. It therefore appears that this linear volcano-tectonic context dominated by fissure eruptions along the rift axis allowed for the development - during the last few hundred thousand years - of successive magma chambers elongated along the same axis with successive rejuvenations though basaltic magma injection from the relatively shallow underlying anomalous mantle.

Geochemical analysis carried on the selected fresh aphyric rock samples provided a complete view of the various kind of liquids emitted during the last million years along this active segment of the rift. The results showed that a very dynamic magmatism had taken place that resulted in differentiation. This is evidenced by the different rock suits noted: basalts, trachytes, and rhyolites. By use of trace elements, it is concluded that the magma sources for the various rock suites are at least three. These is due to the noted different elemental ratios noted in the plotted graphs. Incompatible elements ratios are less affected by FC than other element abundances. They are usually similar in geochemical behaviour and rocks that are related by FC have common/constant ratio. Therefore, the ratio of two incompatible elements in a magma will be more or less the same to that ratio in the magma source, Arevalo and McDonough (2010).

The geological data collected in the field, the rock sample analysis, and the interpretation of the results in terms of geothermal implications have been included in a global geoscientific approach thus allowing for a new conceptual model of the geothermal system in the rift segment to be proposed. As a result of the crystal fractionation and differentiation, this research alludes to magma chamber(s) below the study area. These results are thought to be of interest for the future development of the area, as well as – more generally – the search for new geothermal resources along the East African Rift System away from the central volcanic units along other active rifts segments which represent much wider areas than the ones presently being targeted.

References

[1]. Arevalo, R., and McDonough, W.F. (2010). Chemical variations and regional diversity observed in MORB, Chemical Geology, Volume 271, Issues 1–2, pp70-85.

[2]. Bailey, D.K., (1987). Mantle metasomatism-perspective and prospect, Geological Society, London, Special Publications, 30, pp1-13.

[3]. Barberi, F., Ferrara G., Santacroce R., Treuil M. and Varet J. (1975). A transitional basalt-pantellerite sequence of fractional cristallization, the Boina Centre (Afar Rift, Ethiopia), Journal of Petrology, 16, pp22-56

[4]. Calais, E., Ebinger, C., Hartnady, C. and Nocquet, J. M. (2006). Kinematics of the East African Rift from GPS and earthquake slip vector data. Geological Society, London, Special Publications, 259, pp9-22.

[5]. Chorowicz, J. (2005). The East African Rift System. Journal of African Earth Sciences, 43, pp379–410.

[6]. CIPW Calculations (2018 July 15). Retrieved from: https://www.whitman.edu/geology/winter/Petrology/CIPW Norm Hollacher.xls.

[7]. Clarke, M.C.G., Woodhall, D.G., Allen, D.J., Darling, W.G. (1990). Geological, Volcanological, and Hydrogeological Controls on the Occurrence of Geothermal Activity in the Area Surrounding Lake Naivasha, Kenya. Ministry of Energy, Kenya and British Geological Survey, Nairobi. pp138.

[8]. Hochstaedter, A.G., Gill, J.B., Taylor, B., Ishizuka, O., Yuasa, M., and Morita S., (2000). Across-arc geochemical trends in the Izu-Bonin arc: Constraints on source composition and mantle melting Journal of Geophysical Research, Vol. 105, No. B1, pp495-512.

[9]. LeBas, M.J., LeMaitre, R.W., Streckeisen, A., and Zanettin, B. (1986). A Chemical Classification of Volcanic Rocks Based on the Total Alkali-Silica Diagram. Journal of Petrology, pp27.

[10]. Omenda, P. A. (1997). The Geochemical Evolution of Quaternary Volcanism in the south-central portion of the Kenya Rift. PhD Thesis, University of Texas, El Paso, USA.

[11]. Omenda, P. A., Simiyu S. (2015). Country Update Report for Kenya 2010-2014. Proceedings World Geothermal Congress in Melbourne, Australia.

[12]. Rollinson, H. R., (1993). Using Geochemical Data: Evaluation, Presentation, Interpretation. Pearson Education Ltd., pp 48-49.

Erique O. Nyawir, et. al. "Petrological and Geochemical Evaluation of the Otutu Rift Segment, Kenya."*IOSR Journal of Applied Geology and Geophysics (IOSR-JAGG)*, 10(1), (2022): pp 18-28.